

Mg₃N₂ nanocrystallites formation during the GaN:Mg layers growth by the NH₃-MBE technique

T.V. Malin^a, V.G. Mansurov^a, Yu.G. Galitsyn^a, D.S. Milakhin^a, D.Yu. Protasov^{a,c}, B.Ya. Ber^b, D. Yu. Kazantsev^b, V.V. Ratnikov^b, M.P. Shcheglov^b, A.N. Smirnov^b, V.Yu. Davydov^b, K. S. Zhuravlev^{a,d,*}

^a Physics and Engineering of Semiconductor Structures Department, Rzhanov Institute of Semiconductor Physics, Russian Academy of Sciences, Siberian Branch, Novosibirsk, Russia

^b Ioffe Institute, St. Petersburg 194021, Russia

^c Novosibirsk State Technical University, Novosibirsk 630087, Russia

^d Novosibirsk State University, Novosibirsk 630090, Russia

ARTICLE INFO

Communicated by H. Asahi

Keywords:

A1. Mg₃N₂-crystallites

A3. Ammonia-MBE

B1. p-GaN

B1. GaN:Mg

A1. RHEED

ABSTRACT

The work is devoted to the study of p-GaN: Mg epitaxial layers grown by the ammonia MBE technique. We find that the conductivity of GaN layers doped with Mg does not change with a postgrowth heat treatment. Formation of Mg₃N₂ nanocrystallites on GaN surface during epitaxial growth of the GaN layer with a high magnesium doping level was detected by the RHEED technique for the first time. It was shown that the Mg₃N₂ nanocrystallites formation competes with the acceptor states formation process. It has been proposed that the growth temperature can be applied as an additional “tuning” mechanism which affects the Mg incorporation into the growing GaN:Mg layers.

1. Introduction

A p-type gallium nitride (p-GaN) is widely applied as an operating and contact layer of light-emitting and photodetectors structures based on III-nitrides. Moreover, p-GaN layers are used to create photocathode with negative electron affinity [1] and normally-off transistors [2].

One of the main difficulties in III-nitride technology is obtaining of high-quality layers with the p-type conductivity and high concentration of charge carriers. The problem is caused by the lack of suitable doping impurities for p-GaN layers that would provide shallow donor levels, like boron in silicon or beryllium in gallium arsenide. To obtain the p-type GaN layers the magnesium (Mg) doping is widely used [3]. Significant amount of the incorporated Mg atoms remains often electrically inactive because of hydrogen passivation. Another reason of low hole-carrier concentration in p-type GaN layers is follow. The temperature dependence of the hole concentration studied by the Hall effect had shown that the thermal activation energy of acceptors is in the range of 110–215 meV [4–6]. It means that at room temperature only about 1% of Mg atoms become ionized.

Many ideas proposed by the Nobel laureates S. Nakamura, I. Akasaki

and H. Amano that was formed on the basis of development of the metalorganic chemical vapor deposition (MOCVD) GaN technology are widely accepted. Investigations performed by these authors devoted to development of the light-emitting devices on base of III-nitrides are very significant. They showed that the main form of Mg incorporation into GaN layers is the Mg-H complexes that are electrically inactive. In this case, to make the Mg electrically active as an acceptor, it is required to irradiate samples with low-energy electrons or to apply a post-growth annealing procedure at temperature of about 700 °C [6–10] in a hydrogen-free environment or in vacuum. An increase of the hole-concentration during such post-growth treatments occurs due to a Mg-H complexes destruction and further hydrogen desorption from the epitaxial layer in the result of diffusion process. Later it was found out that the annealing is not required to obtain p-type conductivity in the Mg doped GaN layers (GaN:Mg) grown by both plasma assisted and ammonia molecular beam epitaxy (MBE) [11–13].

An increment of the hole concentration in the GaN epitaxial layer can be achieved by increasing of dopant to main components (Ga and N) fluxes ratio. However, there is a solubility limit of Mg in GaN, which is 10²⁰ cm⁻³. Later it was found, that in parallel to the Mg incorporation

* Corresponding author.

E-mail address: mal-tv@isp.nsc.ru (T.V. Malin).

<https://doi.org/10.1016/j.jcrysgro.2020.125963>

Received 20 August 2020; Received in revised form 13 November 2020; Accepted 17 November 2020

Available online 21 November 2020

0022-0248/© 2020 Published by Elsevier B.V.

process into GaN lattice as an acceptor, the Mg atoms can participate in the formation of another nitride phase, namely Mg_3N_2 . As a result some specific “pyramidal” defects (Mg_3N_2 nanocrystallites) appear in the GaN matrix [14–18]. A negative impact of nanocrystallites formation on the properties of p-doped GaN layers was discussed in [19]. Besides, a high concentration of Mg_3N_2 nanocrystallites can cause a polarity inversion of the GaN epitaxial layer [20,21]. However, an exact form in which the Mg_3N_2 phase (pyramidal defects) is appeared in GaN matrix has not yet been finally established. Literature data indicate that TEM images of Mg_3N_2 inclusions can be interpreted by specialists in the field of TEM in different ways: inversion domain boundaries which consist of Mg_3N_2 building blocks GaN inversion defect (IPD) [17–18,20–21]; hollow defects Mg_3N_2 (empty inside) [15,16]; and precipitates or nanocrystallites [14].

A specific feature was revealed [13,22] during investigation of the p-GaN:Mg growth by the ammonia MBE, namely the p-GaN:Mg layers conductivity decreases with growth temperature increasing. Dussaigne *et al.* believe that this effect may results from an increase in the hydrogen concentration in the samples that was grown at a higher temperature. However, Cristophe *et al.* had systematically studied the impact of the annealing on the GaN:Mg epitaxial layers by Hall measurements and secondary ion mass spectroscopy (SIMS) measurements, and it was shown that this effect is not connected with presence of hydrogen. Hall measurements of the temperature dependence of the holes concentration showed that the samples grown at 840 °C were highly compensated. Consequently, the authors of this work claim that the compensation effect can be explained by the presence of a large number of N vacancies.

The present work is devoted to a comprehensive study of GaN:Mg epitaxial layers grown by ammonia MBE. Formation of Mg_3N_2 nanocrystallites on GaN surface during epitaxial growth of the GaN layer with a high magnesium doping level was detected by the RHEED technique for the first time. This study is aimed to identify the main reasons preventing the increase of the hole concentration with increasing of Mg flux during the p-GaN:Mg growth by the ammonia MBE technique. Besides, the effect of the growth temperature on the holes concentration in GaN:Mg layers is not established now, is still should be clarified.

2. Experimental equipment and samples p-GaN:Mg

The studied series consists of nine samples that include the 1000 nm thick GaN:Mg layer. Samples were grown by ammonia MBE (Riber-32 NH_3) on sapphire substrates over a 300 nm thick AlN buffer layer. The Mg concentration in GaN layer was changed in the range from $8.1 \times 10^{17} \text{ cm}^{-3}$ to $1.5 \times 10^{20} \text{ cm}^{-3}$ by varying of Mg flux. The nitridation conditions of sapphire substrates and the AlN buffer layer growth conditions are described in details elsewhere [23]. The GaN layers were grown at the temperature of 800 °C. The temperature control method is described in details elsewhere [24]. The ammonia flux supplied to the growth chamber was set by the mass flow controller at 200 sccm. The GaN layers were doped by magnesium by using a dual-zone valve solid-state source. Evolution of the surface of GaN samples doped by Mg was studied *in situ* by the reflection high-energy electron diffraction (RHEED) technique using the kSA 400 system for diffraction patterns (DP) processing. The Mg doping level in the samples and the amount of background impurities such as oxygen (O) and/or carbon (C) were determined by Secondary Ion Mass Spectrometry (SIMS). The hole concentration was determined using the Hall effect by the van der Pauw method. The Ohmic contacts preparation to the Hall bridges was performed by using the Ni/Au layers, which allow to lower the potential barrier due to formation of binary intermetallic phases Ni-O/Ni-Ga-O during a burning procedure of the contacts [25]. Edge and screw dislocations densities were determined from X-ray diffraction (XRD) data. Characteristic lines in the Raman spectra (Raman) were used to compare the amount of incorporated Mg into the GaN layers grown under different Mg fluxes.

Percentage, corresponding to a valve opening value of the Mg source,

that controls the magnesium flux, as well as the Mg concentration in the GaN layers, measured using SIMS, and the hole concentration, calculated on the basis of Hall measurements, are given in the Table 1.

3. The effect of sample annealing on the GaN:Mg conductivity

To reveal the post-growth heat treatment effect of the samples on the p-GaN:Mg layers conductivity, prepared by the ammonia MBE, two samples with hole concentrations of $1.9 \times 10^{17} \text{ cm}^{-3}$ and $6.8 \times 10^{17} \text{ cm}^{-3}$ were selected from the grown series. After the Hall bridges formation, the chosen samples were annealed consequently at a temperature of 750 °C in ultrahigh vacuum at a pressure no more than 5.0×10^{-8} Torr for 12 min, 1 h, and 5 h. After each annealing procedure, the Hall measurements were performed repeatedly. On the both samples no any post-growth annealing effect on the hole concentration was found, see Fig. 1. Thus, we can conclude that post-growth heat treatment does not lead to Mg activation, and, therefore, upon GaN layers doping by Mg atoms in the case of ammonia MBE technique, the passivation of the Mg acceptor with hydrogen does not occur.

4. Reflection high energy electron diffraction studies (RHEED)

In situ studies of the GaN epitaxial layer growth process upon Mg doping were performed by the RHEED technique. Fig. 2 (a) shows diffraction patterns (DP) of the non-doped and low Mg-doped ($N_{Mg} < 7.2 \times 10^{19} \text{ cm}^{-3}$) GaN layer surfaces. Such DP with a bright (2×2) reconstruction is typical for GaN layers with metallic polarity [26]. A specific DP of the GaN surfaces of the Mg doped samples in the range of Mg atom concentrations from $3.9 \times 10^{19} \text{ cm}^{-3}$ to $9.5 \times 10^{19} \text{ cm}^{-3}$ is shown in Fig. 2(b). Although the reconstruction spots weaken as the incorporated Mg amount in the GaN film increases, see Fig. 2(b), the presence of the 2×2 reconstruction allows us to conclude that the Ga polarity is maintained when the layers are doped by Mg below the level of $9.5 \times 10^{19} \text{ cm}^{-3}$. Fig. 2(c) corresponds to the specific DP of strongly Mg doped GaN surfaces. The concentration of incorporated Mg into the film for these “magnesium-modified” samples is greater than $1.0 \times 10^{20} \text{ cm}^{-3}$. A DP of the heavily doped GaN:Mg surface has 3D transmission diffraction indications, which are manifested as point spots demonstrating developed 3D surface morphology and does not contain reconstruction spots corresponding to the metallic polarity.

In addition, the appearance of new spots with a periodicity (2.8–2.9 Å) is visible on the DP, which differs from the lateral lattice parameter of the GaN crystal (3.19 Å), that indicates a new crystalline phase formation. The new periodicity agrees well with the known periodicity of the

Table 1

The atomic magnesium and hole concentrations in GaN: Mg layers according to different magnesium fluxes.

Mg flux (valve), %	N_{Mg} , cm^{-3}	p, cm^{-3}
15	8.1×10^{17}	No conductivity
20	1.6×10^{18}	Low conductivity, Hall electromotive force sign corresponds to p-type
23	3.9×10^{19}	1.9×10^{17}
25	5.5×10^{19}	7.8×10^{17}
28	7.2×10^{19}	6.8×10^{17}
30	8.7×10^{19}	6.3×10^{17}
35	9.5×10^{19}	3.1×10^{17}
50	1.5×10^{20}	Low conductivity, no Hall electromotive force
75	1.4×10^{20}	Very low conductivity, no Hall electromotive force

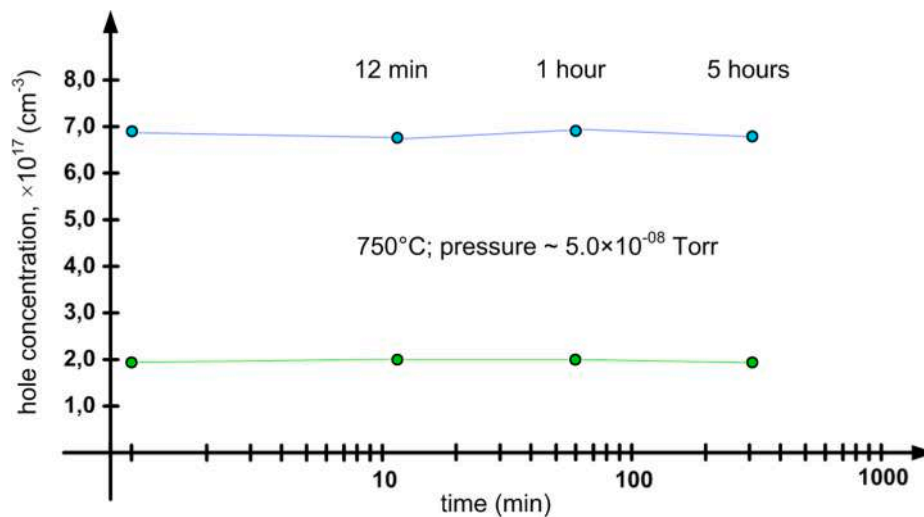


Fig. 1. Dependence of the annealing time influence of p-GaN: Mg layers on the hole concentration.

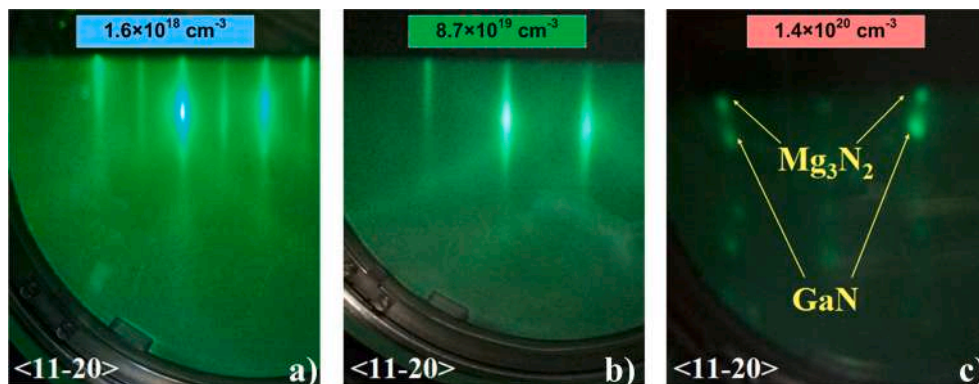


Fig. 2. DP of the GaN epitaxial layer surfaces doped with Mg to different levels, obtained at a temperature of 500 °C in an ammonia flux of 25 sccm.

Mg_3N_2 crystal – $a_{\text{Mg}_3\text{N}_2}/(2\sqrt{3}) = 2.873 \text{ \AA}$ [27], therefore, the newly formed crystalline phase, similarly to authors [18], we associate with the formation of Mg_3N_2 nanocrystallites in GaN layers. These data indicate the existence of a competing mechanism for the Mg atoms incorporation, which can also occur at lower Mg fluxes, however, this competing mechanism is not detectable usually by the RHEED method for the last case.

In order to confirm the detection by the RHEED technique the Mg_3N_2 nanocrystallites formation at high doping level of GaN layers with Mg atoms, experiments dedicated to the crystalline Mg_3N_2 formation on an 350 nm thick AlN buffer layer by the ammonia MBE technique were carried out. AlN layers were grown on a sapphire substrate. The Mg_3N_2 layer was grown at a substrate temperature of 600 °C in the ammonia flux 55 sccm. The Mg flux was provided by the effusion valve source. The reflective DP of the initial AlN surface (a) and the transmission DP after 1.5 h of Mg_3N_2 growth are shown on Fig. 3, demonstrating the stripes from the initial AlN and newly formed crystalline Mg_3N_2 phase (b). Estimation of the newly formed Mg_3N_2 crystalline phase lattice parameter, in terms of the well-known AlN lattice parameter (3.11 Å), gives a value of 2.86 Å, which confirms the conclusion that Mg_3N_2 nanocrystallites are formed on the growing GaN surface in the case of the heavy Mg-doping.

Our RHEED data, namely the observation of transmission diffraction spots, indicate that the Mg_3N_2 phase most likely consists of nanocrystallites with a bulk-like lattice, since transmission diffraction is observed in the case if an electron beam passes through 3D islands. It is important to emphasize that in our case, if Mg_3N_2 were to manifested

exclusively as 2D planar defects (appearing on the inversion domain boundaries of GaN) [17–18,20–21], then the DP would not allow to detect 3D transmission diffraction spots. The bases of the inverted pyramids are parallel to the growth plane (0 0 0 1), so they cannot give transmission diffraction spots on the DP. The faces of the Mg_3N_2 pyramidal inclusions lie on the facets of the IPD and most likely should lead to the appearance of DP with whiskers, similar to the picture corresponding to crystalline quantum dots [28,29]. Our suggestion about formation of the Mg_3N_2 precipitates is in good agreement with the results and model presented in [14].

5. Secondary ion mass spectroscopy (SIMS)

Fig. 4 demonstrates the concentration profiles of magnesium, oxygen, and carbon atoms obtained by SIMS in GaN layers prepared using different opening positions of the valve controlling the Mg flux.

Table 1 shows, that with Mg flux increasing the amount of incorporated to GaN magnesium increases, and as a result, the hole concentration firstly increases. However, the hole concentration decreases at higher fluxes when the threshold value (about $5.5 \times 10^{19} \text{ cm}^{-3}$) is reached. This behavior is consistent with onset of the new Mg_3N_2 phase formation, which was observed by RHEED technique, and indicates that the Mg_3N_2 nanocrystallites formation competes with the incorporation of magnesium into the gallium sites of the GaN crystal lattice, i.e., with the acceptor states formation. In addition, SIMS data show an increase in the background impurities O and C, for the Mg doped GaN layers at concentrations higher than $1.0 \times 10^{20} \text{ cm}^{-3}$. Since the Mg_3N_2 crystalline

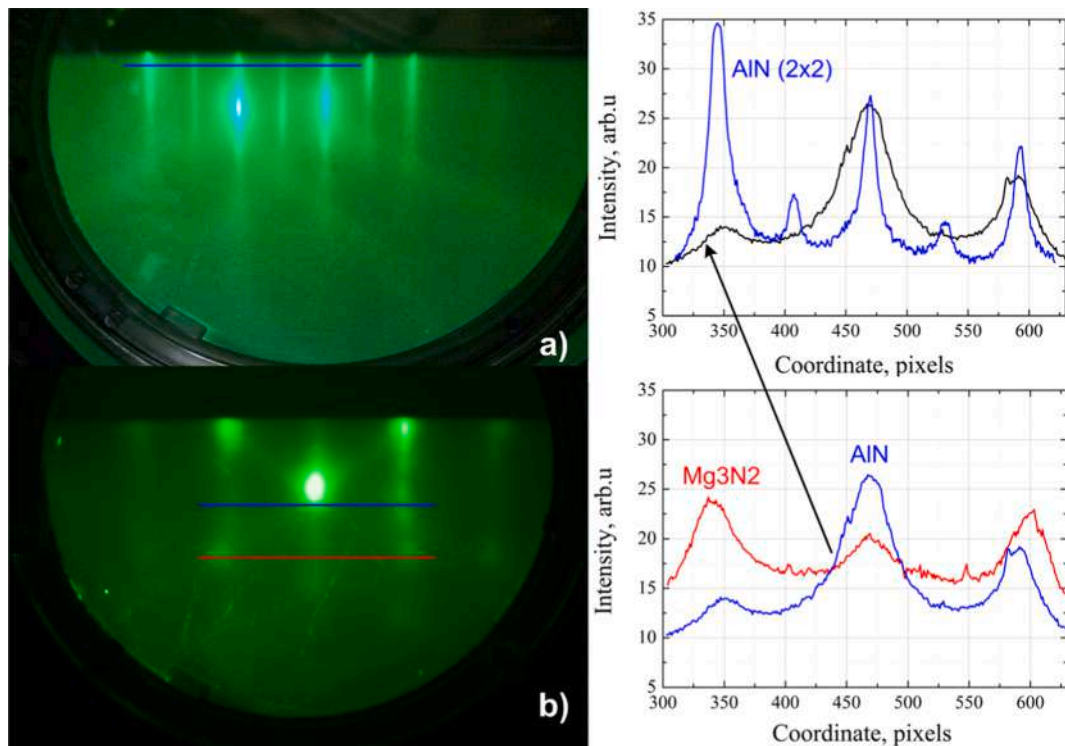


Fig. 3. The DPs and the intensity profiles of the spots glow intensity from the clean AlN surfaces (a) and the newly formed Mg₃N₂ crystalline phase on the AlN surface (b) at a temperature of 600 °C.

phase was detected by RHEED technique only on samples, mentioned above, and according to [20,21], the Mg₃N₂ pyramidal defects can provoke the polarity inversion in the GaN layers. Taking into account the statement of authors of the works [30–32], that the layers grown with nitrogen polarity is characterized by a significantly higher level of background impurities O and C, one can conclude that when doping level in GaN layers increases above the threshold value of $1.0 \times 10^{20} \text{ cm}^{-3}$, the Mg₃N₂ nanocrystallites formation initiates the inversion domains formation with nitrogen polarity in the growing GaN layers and, as a result, the Mg incorporation into the growing layer decreases.

6. Dislocation density

Some selected samples from the grown series were studied by the X-ray diffraction (XRD) method. The full width at half maximum (FWHM) of the symmetric diffraction spot (0 0 0 2), which reflects the micro-orientation of the (0 0 0 1) planes due to defects, mainly, vertical screw dislocations (ρ_{screw}) was measured. The FWHM of the skew-symmetric spot (10–15) (skew-geometry), which is sensitive to displacements, in particular, due to the presence of vertical edge and mixed type of dislocations (ρ_{edge}) was also measured. The dislocation densities were estimated by using the formula of randomly distributed dislocations [33]. The studies showed a sharp dislocations density increasing of both edge and screw types, see Fig. 5, at a Mg doping level in GaN layers above $1.0 \times 10^{20} \text{ cm}^{-3}$, which can be caused by the pyramidal (non point-like) defects appearance associated with the Mg₃N₂ nanocrystallites formation. This behavior is explained by the significant mismatch of lattice parameters for the Mg₃N₂ and the gallium nitride matrix, which is about 9% [27].

7. Raman spectroscopy

The Raman spectra of grown samples series also confirmed the nonlinear behavior of the characteristic peaks associated with Mg atoms incorporation into the films in course of sequential increase in the Mg

flux, as shown in Fig. 6. The high-frequency peak at 2230 cm^{-1} is associated with the Mg-H bond [34]. However, this kind of bonds is not necessarily associated with the Mg acceptor, but may be presented in noticeable amounts in the nanocrystallites of Mg₃N₂ enriched by hydrogen. The increase of intensity of this peak for the samples with a lower doping level is possibly associated with neutral Mg-H complexes. However, the effect of acceptor passivation by the hydrogen, which reduces the hole concentration, has not been manifested itself for our GaN:Mg samples, as it follows from the results of annealing experiments performed for these layers. The effect of post-growth annealing did not been also observed for samples grown by ammonia MBE as was presented by other groups [13,22]. Indeed, the low energy peaks of 260 cm^{-1} and 655 cm^{-1} are related to substitutional Mg dopants according [35], but in addition, these peaks according [36] were also found in Mg₃N₂ material, so increasing of these peaks intensity can be associated with both the Mg acceptor and partially the formation of nanocrystallites Mg₃N₂.

A further increase in the Mg flux leads to the intensities decrease of Mg-related peaks due to a decrease in the number of built-in Mg and a sharp increase in the number of inversion domains in GaN.

8. Lateral biaxial stresses in GaN:Mg layers.

We used the XRD technique to measure the bending radius R, which brings information about homogeneous lateral biaxial compressive stresses σ_a ($R < 0$) or tensile stresses ($R > 0$). The σ_a values were calculated using the Stoney formula [37]; bending of the initial sapphire substrates was taken into account in calculations. Also the stresses in the GaN layer plane were determined by Raman technique using the formula $\sigma_a = \Delta\omega/K$, where $\Delta\omega$ – is the difference between the measured frequency of oscillations of E₂ symmetry phonons (high) and a value of 567.8 cm^{-1} for unstrained GaN [38] and $K = -2.7 \text{ cm}^{-1}\text{GPa}^{-1}$ [38].

Fig. 7 shows the dependences of lateral stresses in GaN: Mg layers as functions of the Mg flux, that was determined by XRD and Raman methods. Both techniques demonstrate very similar stress behavior with

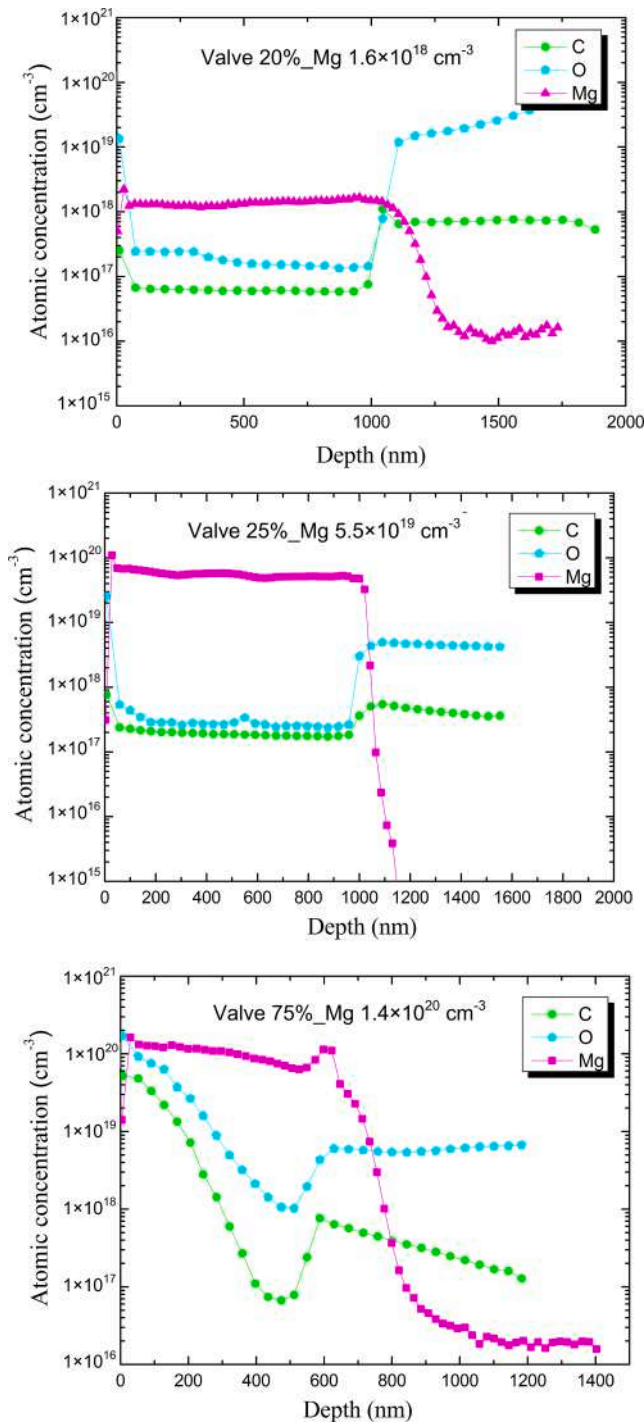


Fig. 4. SIMS profiles of the Mg, C and O atoms concentration in GaN layers with different doping levels.

increasing of the Mg flux, namely elastic compressive stresses in the layers increase with increasing of the Mg doping level. According to data of the both methods, almost complete relaxation of compressive stresses is observed for the GaN: Mg layer grown at the highest Mg flux used here. The increasing of the compressive elastic stresses in GaN at high Mg doping levels was observed in [39,40]. The authors of [40] have reported that there are two thresholds in the elastic stresses behavior: the first threshold was observed at Mg concentration of $7 \times 10^{18} \text{ cm}^{-3}$, where the compressive stresses have changed to tensile stresses, and the second one takes place at Mg concentration of $2 \times 10^{19} \text{ cm}^{-3}$, where opposite behavior was detected (namely, tensile stresses have changed

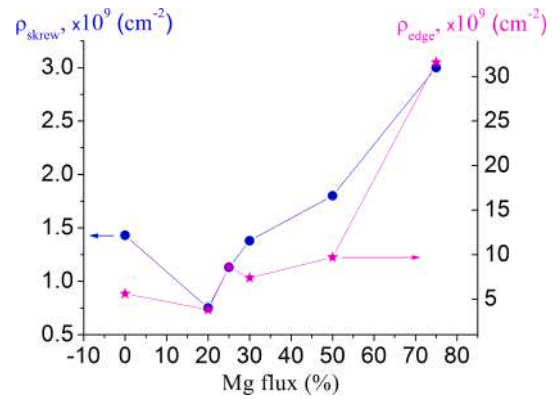


Fig. 5. Dependence of the edge and screw dislocation densities in the GaN: Mg epitaxial layer on the percentage of Mg source valve opening.

to compressive stresses). Kirste et al. have associated the tensile stresses with nitrogen vacancies and the compressive stresses were attributed to Mg-H complexes or the incorporation of other defects such as inversion domains or oxygen. According to the authors of work [39], Mg incorporation into GaN leads to generation of compressive stresses possibly by influencing of Mg on crystal nucleation or by Mg interaction with crystal defects. Since the GaN: Mg layers under the present study were grown on sapphire substrates, the absence of tensile stresses in the sample with a low Mg doping level $N_{\text{Mg}} = 1.6 \times 10^{18} \text{ cm}^{-3}$ can be related to the compensation of tensile stresses by compressive stresses caused by the sapphire substrate [41].

Flynn et al. in their work [39] referencing to the results of calculations performed by the Van de Walle have concluded that the induced compressive stress is not attributable to the size effect of Mg impurity atoms. On the other hand, Lange et al. reported, that at Mg concentrations above $3 \times 10^{18} \text{ cm}^{-3}$, a parasitic Mg_3N_2 phase appears [19]. Hence, the increase in compressive stresses with increasing of the Mg doping level in our case most likely can be associated with the formation of Mg_3N_2 nanocrystallites. In its turn, the almost complete relaxation of the stresses for the sample grown at the Mg flux of 75% (see Fig. 7) can be explained by a sharp increase of the dislocation density in the GaN layer for this extremely high Mg-doping level (see Fig. 5).

9. Growth temperature effect on the GaN layers doping with magnesium

To determine the growth temperature effect on Mg incorporation to the p-GaN:Mg layers, the samples series were grown at both an increased growth temperature of $850 \text{ }^\circ\text{C}$ and a reduced growth temperature of $750 \text{ }^\circ\text{C}$, using three different Mg fluxes corresponding to opening percentages of Mg source valve 15%, 30% and 45%. The conductivity measurements of the samples grown at different temperatures, but under the same Mg fluxes, did not show a systematic change in conductivity depending on the temperature change. So, for samples grown under Mg fluxes corresponding to a 15% valve opening, no changes in the conductivity of the layers were observed either with decreasing or increasing temperature. The samples conductivity measurements grown with Mg fluxes corresponding to a 30% valve opening showed an increase in conductivity with decreasing temperature and a decrease in conductivity with increasing one (in this case, the hole concentrations in the GaN layers were changing to $6.7 \times 10^{17} \text{ cm}^{-3}$ and $5.2 \times 10^{17} \text{ cm}^{-3}$, respectively). The unusual (observed by RHEED) result was obtained during the sample growth under the Mg flux corresponding to 45% valve opening at a growth temperature of $850 \text{ }^\circ\text{C}$. In contrast to the sample grown with the same Mg flux at the temperature of $800 \text{ }^\circ\text{C}$, the diffraction patterns observed after growth are differed radically, see Fig. 8.

The DP of the sample grown at elevated temperature, Fig. 8(b),

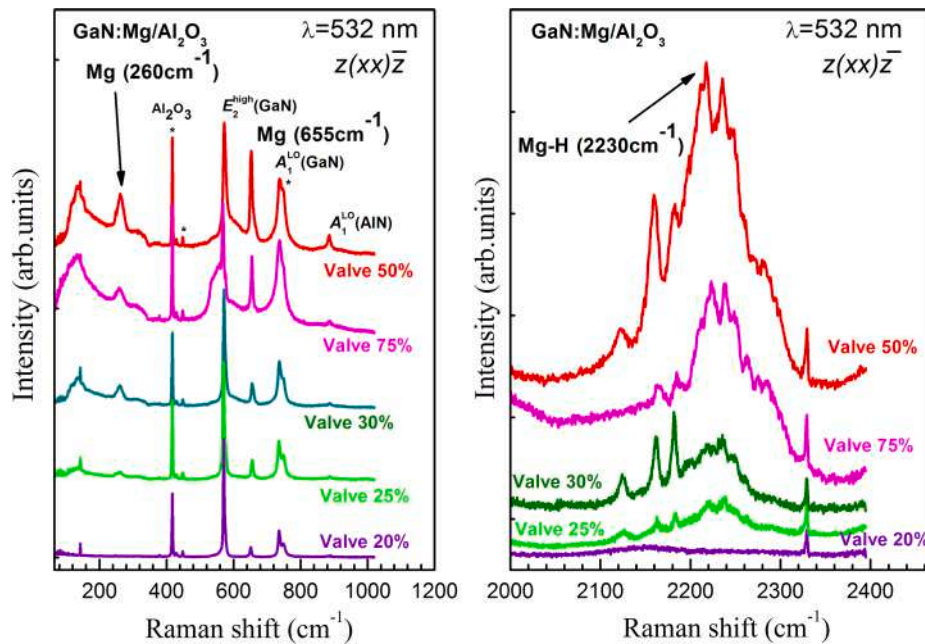


Fig. 6. Raman spectra of GaN:Mg layers.

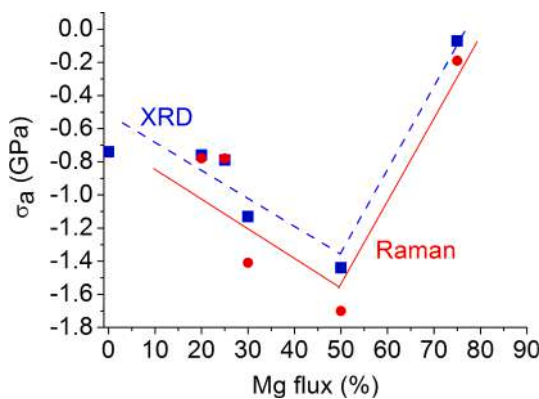


Fig. 7. Dependences of lateral stresses in GaN: Mg layers as a function of Mg flux, determined by the XRD and Raman methods.

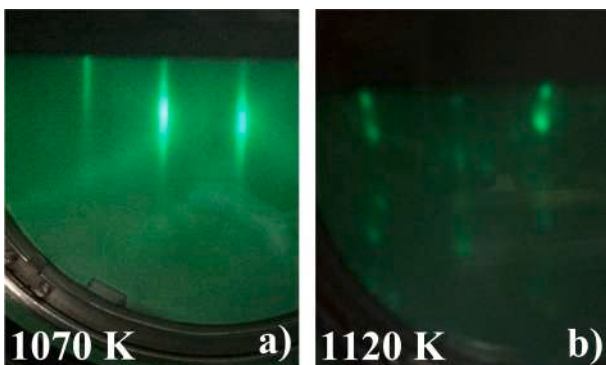


Fig. 8. Diffraction patterns of the GaN:Mg surfaces recorded at a temperature of 500 °C in a 25 sccm ammonia flux. Layers were grown at the temperatures of 800 °C and 850 °C and the Mg flux corresponding to a 45% valve opening.

became exactly the same as for the samples grown with Mg flux corresponding to 50% and 75% valve opening. At the same time, the p-GaN: Mg layer growth at an identical Mg flux, but at the temperature of

800 °C, was characterized by a two-dimensional DP with reconstruction spots, see Fig. 8(a). From our point of view, this observation means that the increase of growth temperature leads to increasing of Ga vacancies concentration in the GaN:Mg layer and, as a consequence, to an increase of incorporated Mg concentration. With a sufficiently large Mg flux, this effect leads to an increase in number of formed Mg_3N_2 nanocrystals, and the RHEED technique allows to detect them, see Fig. 8(b). Thus, the growth temperature can be used as a “tuning” mechanism that affects the Mg incorporation into the growing GaN: Mg layers. At the range of comparatively low Mg fluxes the increase of growth temperature results in the conductivity increasing owing to better Mg incorporation into GaN lattice as an acceptor. The same temperature change for the higher Mg fluxes leads to compensation effect and also leads to a decrease in the fraction of Mg acting as an acceptor due to the formation of Mg_3N_2 nanocrystallites (competing mechanism of Mg consumption). Additional effect that decrease the conductivity of GaN:Mg layers is connected with onset of GaN inversion domains (i.e. with N polarity) stimulated by the Mg_3N_2 nanocrystallites formation.

10. Conclusions

The Mg_3N_2 nanocrystallites formation on the surface of heavily Mg doped GaN layers was detected by the RHEED technique *in situ* for the first time. The Mg_3N_2 nanocrystallites formed at a high doping level lead to a decrease of the hole concentration in the epitaxial GaN layers. The found results can be very useful for the development of MBE growth technology of Mg doped GaN layers. In the case of low conductivity of the GaN epitaxial layers there considering that Mg is a “deep” shallow acceptor, is an intuitive decision to increase the Mg impurity flux to the growing layer that probably is a wrong decision. Relying on the diffraction pattern it is possible to identify *in situ* the Mg_3N_2 nanocrystals formation. As a result it can be established that the reason for the low conductivity of the layers is, in contrast to intuitive impression, the excess Mg flux. The decrease in hole concentration during the Mg_3N_2 nanocrystallites formation in GaN:Mg layers is due to the fact that Mg, which is part of Mg_3N_2 nanocrystallites, does not act as an acceptor. In addition, Mg_3N_2 nanocrystallites stimulate the N-polar inversion domains formation [20,21], which have n-type conductivity and compensate holes in the GaN:Mg layers.

It was established that the amount of Mg incorporated into the

growing GaN film can be affected by the growth temperature variation. The effect is probably connected with the increasing of Ga vacancies concentration resulting from increasing of growth temperature.

CRediT authorship contribution statement

T.V. Malin: Conceptualization, Investigation, Validation, Writing - original draft. **V.G. Mansurov:** Investigation, Visualization, Writing - review & editing. **Yu.G. Galitsyn:** Conceptualization, Methodology, Validation. **D.S. Milakhin:** Investigation, Visualization. **D.Yu. Protasov:** Investigation, Validation. **B.Ya. Ber:** Supervision, Validation. **D. Yu. Kazantsev:** Investigation, Visualization. **V.V. Ratnikov:** Supervision, Validation. **M.P. Shcheglov:** Investigation, Visualization. **A.N. Smirnov:** Investigation, Visualization. **V.Yu. Davydov:** Supervision, Validation. **K.S. Zhuravlev:** Project administration, Funding acquisition, Supervision, Writing - review & editing.

Declaration of Competing Interest

The authors declare that they have no known competing financial interests or personal relationships that could have appeared to influence the work reported in this paper.

Acknowledgements

This study was supported by the Ministry of Science and Higher Education of the Russian Federation as part of state assignment N^o 0306-2019-0008 «Heterostructures based on III-V materials for microwave electronics and microwave photoelectronics» and reported study was funded by RFBR and TUBITAK, project number 21-52-46001. SIMS measurements were performed using the CAMEA IMS7f equipment owned by the Federal Center of Multi-User Equipment “Material Science and Diagnostics for Advanced Technologies” supported by the Ministry of Education and Science of the Russian Federation (RFMEFI62117X0018).

References

- [1] S.A. Rozhkov, V.V. Bakin, D.V. Gorshkov, S.N. Kosolobov, H.E. Scheibler, A. S. Terekhov, Optical phonon cascade emission by photoelectrons at a p-GaN (Cs, O)-vacuum interface, *JETP Lett.* 104 (2) (2016) 135–139, <https://doi.org/10.1134/S0021364016140113>.
- [2] T. Sugiyama, D. Iida, M. Iwaya, S. Kamiyama, H. Amano, I. Akasaki, Threshold voltage control using SiN_x in normally off AlGaIn/GaN HFET with p-GaN gate, *Phys. Status Solidi C* 7 (7–8) (2010) 1980–1982, <https://doi.org/10.1002/pssc.200983595>.
- [3] S. Nakamura, N. Iwasa, M. Senoh, T. Mukai, Compensation mechanism of P-type GaN films, *Jpn. J. Appl. Phys.* 31 (Part 1, No. 5A) (1992) 1258–1266, <https://doi.org/10.1143/JJAP.31.1258>.
- [4] P. Kozodoy, H. Xing, S.P. DenBaars, U.K. Mishra, A. Saxler, R. Perrin, S. Elhamri, W.C. Mitchel, Heavy doping effects in Mg-doped Ga, *J. Appl. Phys.* 87 (4) (2000) 1832–1835, <https://doi.org/10.1063/1.372098>.
- [5] I. Akasaki, H. Amano, Widegap column-III nitride semiconductors for UV/blue light emitting devices, *J. Electrochem. Soc.* 141 (8) (1994) 2266, <https://doi.org/10.1149/1.2055104>.
- [6] W. Gotz, N.M. Johnson, J. Walker, D.P. Bour, Activation of acceptors in Mg-doped, p-Type GaN, *Mater. Res. Soc. Symp. Proc.* 423 (1996) 595–600, <https://doi.org/10.1557/PROC-423-595>.
- [7] H. Amano, M. Kito, K. Hiramatsu, I. Akasaki, P-type conduction in Mg-doped GaN treated with low-energy electron beam irradiation (LEEBI), *Jpn. J. Appl. Phys.* 28 (Part 2, No. 12) (1989) L2112–L2114, <https://doi.org/10.1143/JJAP.28.L2112>.
- [8] S. Nakamura, T. Mukai, M. Senoh, N. Iwasa, Thermal annealing effects on P-type Mg-doped GaN films, *Jpn. J. Appl. Phys.* 31 (Part 2, No. 2B) (1992) L139–L142, <https://doi.org/10.1143/JJAP.31.L139>.
- [9] D.H. Youn, M. Lachab, M. Hao, T. Sugahara, H. Takenaka, Y. Naoi, S. Sakai, Investigation on the P-type activation mechanism in Mg-doped GaN films grown by metalorganic chemical vapor deposition, *Jpn. J. Appl. Phys.* Part 1 38 (Part 1, No. 2A) (1999) 631–634, <https://doi.org/10.1143/JJAP.38.631>.
- [10] N.M. Johnson, W. Gotz, J. Neugebauer, C.G. Van de Walle, Hydrogen in GaN, *Mater. Res. Soc. Symp. Proc.* 395 (1996) 723–732, <https://doi.org/10.1557/PROC-395-723>.
- [11] W. Kim, A. Salvador, A.E. Botchkarev, O. Aktas, S.N. Mohammad, H. Morkoc, Mg-doped p-type GaN grown by reactive molecular beam epitaxy, *Appl. Phys. Lett.* 69 (4) (1996) 559–561, <https://doi.org/10.1063/1.117786>.
- [12] J.M. Myoung, K.H. Shim, O. Gluschenkov, C. Kim, K. Kim, S. Kim, S.G. Bishop, Effect of growth temperature on the properties of p-type GaN grown by plasma-assisted molecular beam epitaxy, *J. Cryst. Growth* 182 (3–4) (1997) 241–246, [https://doi.org/10.1016/S0022-0248\(97\)00380-1](https://doi.org/10.1016/S0022-0248(97)00380-1).
- [13] C.A. Hurni, J.R. Lang, P.G. Burke, J.S. Speck, Effects of growth temperature on Mg-doped GaN grown by ammonia molecular beam epitaxy, *Appl. Phys. Lett.* 101 (10) (2012) 102106, <https://doi.org/10.1063/1.4751108>.
- [14] M. Hansen, L.F. Chen, J.S. Speck, S.P. DenBaars, Observation of Mg-rich precipitates in the p-type doping of GaN-based laser diodes, *Phys. Status Solidi B* 228 (2) (2001) 353–356, [https://doi.org/10.1002/1521-3951\(200111\)228:2<353::AID-PSSB353>3.0.CO;2-Q](https://doi.org/10.1002/1521-3951(200111)228:2<353::AID-PSSB353>3.0.CO;2-Q).
- [15] Z. Liliental-Weber, M. Benamara, J. Wasburn, I. Grzegory, S. Porowski, Spontaneous ordering in bulk GaN: Mg samples, *Phys. Rev. Lett.* 83 (12) (1999) 2370–2373, <https://doi.org/10.1103/PhysRevLett.83.2370>.
- [16] Z. Liliental-Weber, M. Benamara, J. Swider, J. Wasburn, I. Grzegory, S. Porowski, D.J.H. Lambert, C.J. Eiting, R.D. Dupuis, Mg-doped GaN: Similar defects in bulk crystals and layers grown on Al₂O₃ by metal-organic chemical-vapor deposition, *Appl. Phys. Lett.* 75 (26) (1999) 4159–4161, <https://doi.org/10.1063/1.125568>.
- [17] P. Vennegues, M. Benaissa, B. Beaumont, E. Feltn, P. De Mierry, S. Dalmasso, M. Leroux, P. Gibart, Pyramidal defects in metalorganic vapor phase epitaxial Mg doped GaN, *Appl. Phys. Lett.* 77 (6) (2000) 880–882, <https://doi.org/10.1063/1.1306421>.
- [18] P. Vennegues, M. Leroux, S. Dalmasso, M. Benaissa, P. De Mierry, P. Lorenzini, B. Damilano, B. Beaumont, J. Massies, P. Gibart, Atomic structure of pyramidal defects in Mg-doped GaN, *Phys. Rev. B* 68 (23) (2003) 235214, <https://doi.org/10.1103/physrevb.68.235214>.
- [19] B. Lange, Ch. Freysoldt, J. Neugebauer, Native and hydrogen-containing point defects in Mg₃N₂: a density functional theory study, *Phys. Rev. B* 81 (2010) 224109, <https://doi.org/10.1103/PhysRevB.81.224109>.
- [20] S. Pezzagna, P. Vennegues, N. Grandjean, J. Massies, Polarity inversion of GaN(0 0 1) by a high Mg doping, *J. Cryst. Growth* 269 (2004) 249–256, <https://doi.org/10.1016/j.jcrysgro.2004.05.067>.
- [21] V. Ramachandran, R.M. Feenstra, W.L. Sarney, L. Salamanca-Riba, J.E. Northrup, L.T. Romano, D.W. Greve, Inversion of wurtzite GaN(0001) by exposure to magnesium, *Appl. Phys. Lett.* 75 (6) (1999) 808–810, <https://doi.org/10.1063/1.124520>.
- [22] A. Dussaigne, B. Damilano, J. Brault, J. Massies, E. Feltn, N. Grandjean, High doping level in Mg-doped GaN layers grown at low temperature, *J. Appl. Phys.* 103 (1) (2008) 013110, <https://doi.org/10.1063/1.2829819>.
- [23] T.V. Malin, D.S. Milakhin, V.G. Mansurov, Yu.G. Galitsyn, A.S. Kozhuhov, V. V. Ratnikov, A.N. Smirnov, V.Yu. Davydov, K.S. Zhuravlev, Effect of the sapphire-nitridation level and nucleation-layer enrichment with aluminum on the structural properties of AlN layers, *Semiconductors* 52 (6) (2018) 789–796, <https://doi.org/10.1134/S1063782618060143>.
- [24] T.V. Malin, V.G. Mansurov, A.M. Gilinskii, D.Yu. Protasov, A.S. Kozhukhov, A. P. Vasilenko, K.S. Zhuravlev, Growth of AlGaIn/GaN heterostructures with a two-dimensional electron gas on AlN/Al₂O₃ substrates, *Optoelectronics, Instrum. Data Process.* 49 (5) (2013) 429–433, <https://doi.org/10.3103/S8756699013050026>.
- [25] J.-K. Ho, C.-S. Jong, C.C. Chiu, C.-N. Huang, K.-K. Shih, L.-C. Chen, F.-R. Chen, J.-J. Kai, Low-resistance ohmic contacts to p-type GaN achieved by the oxidation of Ni/Au films, *J. Appl. Phys.* 86 (8) (1999) 4491–4497, <https://doi.org/10.1063/1.371392>.
- [26] A.R. Smith, R.M. Feenstra, D.W. Greve, M.-S. Shin, M. Skowronski, J. Neugebauer, J.E. Northrup, GaN(0001) surface structures studied using scanning tunneling microscopy and first-principles total energy calculations, *Surf. Sci.* 423 (1) (1999) 70–84, [https://doi.org/10.1016/S0039-6028\(98\)00903-0](https://doi.org/10.1016/S0039-6028(98)00903-0).
- [27] W. Paszkowicz, M. Knapp, J.Z. Domagala, G. Kamler, S. Podsiadlo, Low-temperature thermal expansion of Mg₃N₂, *J. Alloy. Compd.* 328 (1–2) (2001) 272–275, [https://doi.org/10.1016/S0925-8388\(01\)01310-X](https://doi.org/10.1016/S0925-8388(01)01310-X).
- [28] B. Damilano, J. Brault, J. Massies, Formation of GaN quantum dots by molecular beam epitaxy using NH₃ as nitrogen source, *J. Appl. Phys.* 118 (2015) 024304, <https://doi.org/10.1063/1.4923425>.
- [29] K.A. Konfederatova, V.G. Mansurov, T.V. Malin, Y.G. Galitsyn, I.A. Aleksandrov, V. I. Vdovin, K.S. Zhuravlev, Role of the phase transition at GaN QDs formation on (0001)AlN surface by ammonia molecular beam epitaxy, *J. Therm. Anal. Calorim.* 133 (2) (2018) 1181–1187, <https://doi.org/10.1007/s10973-018-7280-1>.
- [30] R. Collazo, S. Mita, J. Xie, A. Rice, J. Tweedie, R. Dalmau, Z. Sitar, Implementation of the GaN lateral polarity junction in a MESFET utilizing polar doping selectivity, *Phys. Status Solidi A* 207 (1) (2010) 45–48, <https://doi.org/10.1002/pssa.200982629>.
- [31] M.N. Fireman, H. Li, S. Keller, U.K. Mishra, J.S. Speck, Growth of N-polar GaN by ammonia molecular beam epitaxy, *J. Cryst. Growth* 481 (2018) 65–70, <https://doi.org/10.1016/j.jcrysgro.2017.10.033>.
- [32] T. Tanikawa, S. Kuboya, T. Matsuoka, Control of impurity concentration in N-polar (0001) GaN grown by metalorganic vapor phase epitaxy, *Phys. Status Solidi B* 254 (8) (2017) 1600751, <https://doi.org/10.1002/pssb.201600751>.
- [33] C.G. Dunn, E.F. Koch, Comparison of dislocation densities of primary and secondary recrystallization grains of Si-Fe, *Acta Metall.* 5 (10) (1957) 548–554, [https://doi.org/10.1016/0001-6160\(57\)90122-0](https://doi.org/10.1016/0001-6160(57)90122-0).
- [34] M.S. Brandt, J.W. Ager, W. Gotz, N.M. Johnson, J.S. Harris, R.J. Molnar, T. D. Moustakas, Local vibrational modes in Mg-doped gallium nitride, *Phys. Rev. B* 49 (20) (1994) 14758–14761, <https://doi.org/10.1103/physrevb.49.14758>.
- [35] G. Kaczmarczyk, A. Kaschner, A. Hoffmann, C. Thomsen, Impurity-induced modes of Mg, As, Si, and C in hexagonal and cubic GaN, *Phys. Rev. B* 61 (8) (1999) 5353–5357, <https://doi.org/10.1103/physrevb.61.5353>.

- [36] M. Anton, Heyns, Linda C. Prinsloo, Klaus-Jurgen Range, Martin Stassen, The vibrational spectra and decomposition of α -calcium nitride (α -Ca₃N₂) and magnesium nitride (Mg₃N₂), *J. Solid State Chem.* 137 (1998) 33–41, <https://doi.org/10.1006/jssc.1997.7672>.
- [37] G.G. Stoney, The tension of metallic films deposited by electrolysis, *Proc. Royal Soc. London* 82 (553) (1909) 172–175, <https://doi.org/10.1098/rspa.1909.0021>.
- [38] V.Yu. Davydov, N.S. Averkiev, I.N. Goncharuk, D.K. Nelson, I.P. Nikitina, A. S. Polkovnikov, A.N. Smirnov, M.A. Jacobson, O.K. Semchinova, Raman and Photoluminescence studies of biaxial strain in GaN epitaxial layers grown on 6H-SiC, *J. Appl. Phys.* 82 (1997) 5097–5102, <https://doi.org/10.1063/1.366310>.
- [39] C. Flynn, W. Lee, The dependence of Raman scattering on Mg concentration in Mg-doped GaN grown by MBE, *Mater. Res. Express* 1 (2014) 025901, <https://doi.org/10.1088/2053-1591/1/2/025901>.
- [40] R. Kirste, M.P. Hoffmann, J. Tweedie, Z. Bryan, G. Callsen, Ch. Thomas Kure, M. R. Nenstiel, R. Collazo Wagner, Hoffmann Ax, Zlatko Sitar, Compensation effects in GaN: Mg probed by Raman spectroscopy and photoluminescence measurements, *J. Appl. Phys.* 113 (1997) 103504, <https://doi.org/10.1063/1.4794094>.
- [41] C. Kisielowski, J. Kruger, S. Ruvimov, T. Suski, J.W. Ager III, E. Jones, Z.L. Weber, M. Rubin, E.R. Weber, M.D. Bremser, R.F. Davis, Strain-related phenomena in GaN thin films, *Phys. Rev. B* 54 (24) (1996) 17745–17753, <https://doi.org/10.1103/PhysRevB.54.17745>.